

## Hydrogen Adsorption in a Highly Stable Porous Rare-Earth Metal-Organic Framework: Sorption Properties and Neutron Diffraction Studies

Junhua Luo,<sup>\*,†</sup> Hongwu Xu,<sup>†,‡</sup> Yun Liu,<sup>§,¶</sup> Yusheng Zhao,<sup>\*,†</sup> Luke L. Daemen,<sup>†</sup> Craig Brown,<sup>§</sup> Tatiana V. Timofeeva,<sup>#</sup> Shengqian Ma,<sup>⊥</sup> and Hong-Cai Zhou<sup>⊥</sup>

LANSCCE-12 and EES-6, Los Alamos National Laboratory, Los Alamos, New Mexico 87545, NIST Center for Neutron Research, Gaithersburg, Maryland 20899, Department of Materials Science and Engineering, University of Maryland, College Park, Maryland 20742, Department of Natural Sciences, New Mexico Highlands University, Las Vegas, New Mexico 87701, and Department of Chemistry & Biochemistry, Miami University, Oxford, Ohio 45056

Received February 25, 2008; E-mail: jhluo@lanl.gov; yzhao@lanl.gov

Storage and distribution of hydrogen are key enabling technologies for a future hydrogen economy,<sup>1</sup> especially, the hydrogen storage aspect poses the biggest challenge to current materials and technologies.<sup>2–3</sup> Many types of materials have been considered, including carbon nanotubes (CNTs),<sup>4</sup> activated carbons,<sup>5</sup> metal hydrides,<sup>6</sup> and hydrogen clathrates.<sup>7</sup> In contrast to other materials, metal-organic frameworks (MOFs) have well-defined crystal structures with system pores of uniform pore size (about 0.5–2 nm in diameter), and moreover, the variety of possible topologies and chemical compositions enables rational design and syntheses of MOFs to optimize hydrogen adsorption properties.<sup>8–10</sup> A fundamental understanding of the hydrogen adsorption behaviors is essential to optimize the performance of MOFs for hydrogen storage. While there are numerous extensive studies for TMOFs (transitional metal-organic frameworks),<sup>11–13</sup> there are no experimental data regarding the hydrogen adsorption mechanisms and behaviors in RMOFs (rare-earth metal-organic frameworks). Such fundamental studies are essential for the optimization of this new class of rare-earth metal-organic framework materials for practical hydrogen storage applications. We present our studies of the gas sorption properties of a porous rare-earth metal-organic framework, Y(BTC)(H<sub>2</sub>O)•4.3H<sub>2</sub>O (**1**) (H<sub>3</sub>BTC = 1,3,5-benzenetricarboxylate), synthesized by solvothermal reaction. The dehydrated sample (**1a**) exhibits permanent porosity, selective gas adsorption, and good H<sub>2</sub> adsorption ability. We used powder neutron diffraction to demonstrate for the first time direct structural evidence that an optimal pore size (around 6 Å) strengthens the interactions between H<sub>2</sub> molecules with pore walls, which thereby allows for enhancing hydrogen adsorption from the interaction between hydrogen molecules with the pore walls rather than with the open metal sites within the framework.

The composition and crystal structure of compound **1**, Y(BTC)(H<sub>2</sub>O)•4.3H<sub>2</sub>O, were determined by single-crystal X-ray diffraction, TGA and elemental analysis studies (see Supporting Information). The X-ray structural analysis reveals that Y atoms are bridged by a BTC linker to form a tetragonal porous framework with channels about 5.8 × 5.8 Å<sup>2</sup> along the *c* axis (Figure 1). TGA result indicates **1** is stable up to 490 °C, and the framework is retained after thermal activation (compound **1a**). The permanent porosity of **1a** has been confirmed by N<sub>2</sub> and H<sub>2</sub> gas sorption measurement at 77 K. Sorption studies show that **1a** can take up a moderate amount of hydrogen at 1 atm and 77 K [176 cm<sup>3</sup> g<sup>-1</sup>

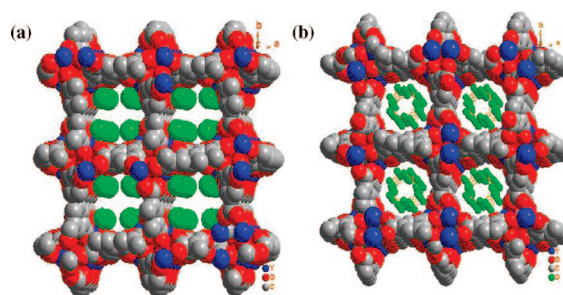


**Figure 1.** (a) Porous structure of **1** with coordinated water molecules (green) inside, and (b) hydrogen clusters formed inside **1a**.

(STP), 1.57 wt %], exhibiting highly selective sorption of hydrogen over nitrogen gas molecules. The 77 and 87 K isotherms were fit to determine the isosteric heat of adsorption using a virial equation. The enthalpy of adsorption for **1a** reaches almost 7.3 kJ mol<sup>-1</sup>, which is comparable to the value for the nanoporous prussian blue compounds with open transitional metal sites<sup>17</sup> and the hyper-cross-linked organic polymer and nanoporous slit-like carbon.<sup>18,19</sup> High pressure hydrogen adsorption isotherms of **1a** were measured at 77 and 87 K (see Supporting Information). At 77 K, the sorption isotherm has a type I profile, saturated at 10 bar with a hydrogen uptake of ~2.1 wt %, which is comparable to those found in other MOFs (e.g., 2.3 wt % in MOF-74).<sup>20</sup> The volumetric hydrogen storage is 28.8 g/L at 77 K and 10 bar.

Powder neutron diffraction data were collected on the high-resolution neutron powder diffractometer (BT-1) at the NCNR of NIST. Figure S5a in the Supporting Information plots the neutron diffraction pattern of the Y(BTC) bare material measured at 4 K. The refined lattice parameters and atomic positions of Y, C, and O atoms agree well with the room-temperature single-crystal XRD results. Differences in the neutron diffraction patterns recorded upon charging the sample of **1a** with approximately 0.64(5), 1.32(3), 2.11(7), 2.95(8), 4.23(8), and 5.53(3) D<sub>2</sub> per Y(BTC) formula unit were used to identify the successive hydrogen binding sites within the framework. One H<sub>2</sub>/Y corresponds to ~0.68 wt % hydrogen uptake. Rietveld analyses of the 4.2D<sub>2</sub>:Y loaded sample revealed the location of 4 D<sub>2</sub> adsorption sites, each site representing the centroid of the D<sub>2</sub> molecule (Figure 2). The difference Fourier nuclear map obtained with a loading of 0.64(5) D<sub>2</sub> molecules per formula unit clearly identifies the position of the first adsorption site (Figure 3). Surprisingly, the D<sub>2</sub> centroid of the strongest adsorption position, site I (corner site I), is not directly coordinated to the open metal Y ion like the other reported MOFs<sup>11,12</sup> but is associated with the aromatic BTC linker, at a distance of 4.27 Å from the exposed Y<sup>3+</sup> ions and 3.7 Å from the benzene rings of

<sup>†</sup> LANSCCE-12, Los Alamos National Laboratory.

<sup>‡</sup> EES-6, Los Alamos National Laboratory.

<sup>§</sup> NIST Center for Neutron Research.

<sup>¶</sup> University of Maryland.

<sup>#</sup> New Mexico Highlands University.

<sup>⊥</sup> Miami University.

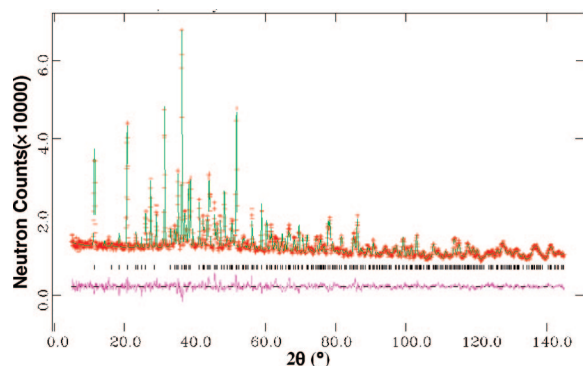


**Figure 2.** Rietveld analysis of powder neutron diffraction data of **1a** with a hydrogen loading of 4.2 H<sub>2</sub>/Y: observed (red dots), refined (green line), difference (pink line), and allowed reflections (black tick marks).

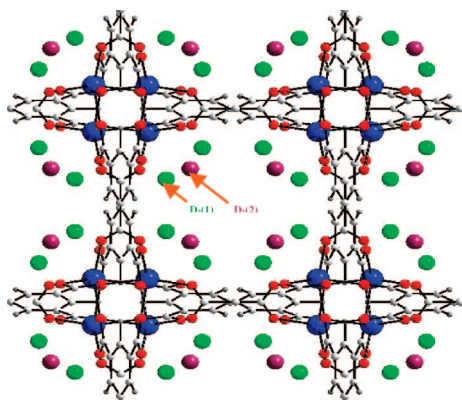


**Figure 3.** First and second H<sub>2</sub> adsorption sites in **1a**.

the BTC linkers within the framework. This result provides for the first time direct structural evidence for the recent findings that small pores with an optimal pore diameter of just slightly over twice the kinetic diameter of the hydrogen molecules (i.e., a pore diameter of about 6–7 Å) strengthen the interactions between H<sub>2</sub> molecules with pore walls and thus increase the heat of hydrogen adsorption.<sup>14–16</sup> Ideally, all adsorbed hydrogen molecules should interact directly with adsorbing centers located in the pores walls (i.e., monolayer adsorption). Evidently, this optimal pore size results in stronger total van der Waals interactions between H<sub>2</sub> molecules and pore walls, and such interactions strongly compete with the interactions between the H<sub>2</sub> molecules with the open Y<sup>3+</sup> ions. Importantly, at an increased D<sub>2</sub> loading of 2.11(7) D<sub>2</sub> molecules per formula unit, adsorption at site I in **1a** approaches saturation, with a site occupancy of 92%.

Three additional D<sub>2</sub> adsorption sites were also identified in **1a**. The order of filling of subsequent sites is sequential from D<sub>2</sub>(2) to D<sub>2</sub>(4). Following the first strong binding site D<sub>2</sub>(1), there is a progressive occupation of the D<sub>2</sub>(2) site (corner site II), which lies in the middle of the corners within the pores at a closer distance of 3.9 Å from the open Y ion and a distance of 3.6 Å from the benzene ring of the BTC unit. D<sub>2</sub> molecules in site III, which is comparable to site II in binding energy, are situated with their centroids 4.3 Å from the Y atoms and 2.96 Å from six BTC oxygen atoms, and within van der Waals contact of the planes of 3.8 Å from the BTC carbon atoms. With further D<sub>2</sub> loading, the first three adsorption sites were almost completely occupied. The fourth site is considerably weaker in binding energy and only becomes occupied at high loadings. Analysis of the 4.23(8) D<sub>2</sub>:Y phase reveals that D<sub>2</sub>(4) lies 3.31(1) Å from two BTC carboxylate carbon atoms and 3.23(1)

Å from two BTC carboxylate oxygen atoms. Interestingly, the first three adsorption sites discussed above form a nanocage within **1a**, and the nearest neighbor distances between these adsorption sites are about 2.86 Å (Figure 1). This distance is even shorter than the 3.6 Å of solid H<sub>2</sub>, implying a significant pressurizing effect of the framework on the encapsulated hydrogen molecules.<sup>13,21</sup>

In conclusion, a highly stable porous lanthanide metal-organic framework, Y(BTC)(H<sub>2</sub>O)·4.3H<sub>2</sub>O (BTC = 1,3,5-benzenetricarboxylate), exhibiting highly selective sorption behaviors of hydrogen over nitrogen gas molecules, has been constructed and investigated for hydrogen storage. We obtained detailed structural information including H<sub>2</sub> adsorption sites and binding energies in a rare-earth MOF structure for the first time. Moreover, powder neutron diffraction studies provide for the first time direct structural evidence demonstrating that an optimal pore size (~6 Å) strengthens the interactions between H<sub>2</sub> molecules with pore walls and allows for enhancing hydrogen adsorption from the interaction between hydrogen molecules with the pore walls rather than with the open metal sites within the framework. Four distinct D<sub>2</sub> sites were located and found to be progressively filled within the nanopore structure. At high concentration of hydrogen loading, Y(BTC) is able to hold hydrogen molecules up to 3.7 wt % as self-assembled nanostructures with relatively short intermolecular distances.

**Acknowledgment.** This work was funded by a LDRD project, Los Alamos National Laboratory is operated by Los Alamos National Security, LLC, under DOE Contract DE-AC52-06NA25396.

**Supporting Information Available:** Powder X-ray diffraction, X-ray crystallographic file, TGA, detailed information about the Rietveld refinements and the crystallographic data for Y(BTC)-*n*D<sub>2</sub> (*n* = 0, 0.64(5), 1.32(3), 2.11(7), 2.95(8), 4.23(8), and 5.53(3)), and other detailed experimental information. This material is available free of charge via the Internet at <http://pubs.acs.org>.

## References

- (1) Coontz, R.; Hanson, B. *Science* **2004**, *305*, 957 (Towards a hydrogen economy, special issue).
- (2) Service, R. F. *Science* **2004**, *305*, 958–961.
- (3) Zuttel, A. *Mater. Today* **2003**, *6*, 24–33.
- (4) Cheng, H.; Pez, G. P.; Cooper, A. C. *J. Am. Chem. Soc.* **2001**, *123*, 5845–5846.
- (5) Gogotsi, Y.; Nikitin, A.; Ye, H.; Zhou, W.; Fischer, J. E.; Yi, B.; Foley, H. C.; Barsoum, M. W. *Nat. Mater.* **2003**, *2*, 591–594.
- (6) Schimmel, H. G.; Huot, J.; Chapon, L. C.; Tichelaar, F. D.; Mulder, F. M. *J. Am. Chem. Soc.* **2005**, *127*, 14348–14354.
- (7) Struzhkin, V. V.; Miltzer, B.; Mao, W. L.; Mao, H.-k.; Hemley, R. J. *Chem. Rev.* **2007**, *107*, 4133–4151.
- (8) Rosi, N. L.; Eckert, J.; Eddaoudi, M.; Vodak, D. T.; Kim, J.; O’Keeffe, M.; Yaghi, O. M. *Science* **2003**, *300*, 1127–1129.
- (9) Ma, S.; Sun, D.; Ambrogio, M.; Fillinger, J. A.; Parkin, S.; Zhou, H.-C. *J. Am. Chem. Soc.* **2007**, *129*, 1858–1859.
- (10) Dinca, M.; Yu, A. F.; Long, J. R. *J. Am. Chem. Soc.* **2006**, *128*, 8904–8913.
- (11) Peterson, V. K.; Liu, Y.; Brown, C. M.; Kepert, C. J. *J. Am. Chem. Soc.* **2006**, *128*, 15578–15579.
- (12) Dinca, M.; Dailly, A.; Liu, Y.; Brown, C. M.; Neumann, D. A.; Long, J. R. *J. Am. Chem. Soc.* **2006**, *128*, 16876–16883.
- (13) Wu, H.; Zhou, W.; Yildirim, T. *J. Am. Chem. Soc.* **2007**, *129*, 5314–5315.
- (14) Gogotsi, Y.; Dash, R. K.; Yushin, G.; Yildirim, T.; Laudisio, G.; Fischer, J. E. *J. Am. Chem. Soc.* **2005**, *127*, 16006–16007.
- (15) Yushin, G.; Dash, R.; Jagiello, J.; Fischer, J. E.; Gogotsi, Y. *Adv. Funct. Mater.* **2006**, *16*, 2288–2293.
- (16) Yang, Z.; Xia, Y.; Mokaya, R. *J. Am. Chem. Soc.* **2007**, *129*, 1683–1679.
- (17) Kaye, S. S.; Long, J. R. *J. Am. Chem. Soc.* **2005**, *127*, 6506–6507.
- (18) Wood, C. D.; Tan, B.; Trewin, A.; Niu, H.; Bradshaw, D.; Rosseinsky, M. J.; Khimyak, Y. Z.; Campbell, N. L.; Kirk, R.; Stöckel, E.; Cooper, A. I. *Chem. Mater.* **2007**, *19*, 2034–2048.
- (19) Kowalczyk, P.; Gauden, P. A.; Terzyk, A. P.; Bhatia, S. K. *Langmuir* **2007**, *23*, 3666–3672.
- (20) Wong-Foy, A. G.; Matzger, A. J.; Yaghi, O. M. *J. Am. Chem. Soc.* **2006**, *128*, 3494–3495.
- (21) Yildirim, T.; Hartman, M. R. *Phys. Rev. Lett.* **2005**, *95*, 215504–215507.

JA801411F